Macalester Journal of Physics and Astronomy

Volume 4
Issue 1 *Spring 2016*

Article 9

May 2016

Power and Langmuir Probe Measurements of H2 RF Plasma

Alexander A. Stowell
Macalester College, astowell@macalester.edu

Abstract

Methane based gases are often used to produce thin films of biomaterials, such as diamond-like carbon, through Plasma Enhanced Chemical Vapor Deposition. The characterization of the H_2 plasma will give a deeper understanding of the physical processes occurring. Understanding these processes could lead to the optimization of the production of these thin films in the future. In this paper, we examine the H_2 plasma using a Langmuir probe to gain information on the electron temperature and density of the plasma discharge. We measured electron temperatures of 6eV. Our Langmuir probe data indicates the electron temperature remains constant as the power is increased and the additional energy is used to increase the plasma density at a rate proportional to the increase in power.

Power and Langmuir Probe Measurements of H2 RF Plasma

Cover Page Footnote
Professor James Doyle for the research opportunity and all of the assistance and guidance.

Power and Langmuir Probe Measurements of H_2 RF Plasma

Zandy Stowell, John Carlson
Advisor: James Doyle
Dept. of Physics and Astronomy, Macalester College

ABSTRACT

Methane based gases are often used to produce thin films of biomaterials, such as diamond-like carbon, through Plasma Enhanced Chemical Vapor Deposition. The characterization of the H_2 plasma will give a deeper understanding of the physical processes occurring. Understanding these processes could lead to the optimization of the production of these thin films in the future. In this paper, we examine the H_2 plasma using a Langmuir probe to gain information on the electron temperature and density of the plasma discharge. We measured electron temperatures of 6eV. Our Langmuir probe data indicates the electron temperature remains constant as the power is increased and the additional energy delivered to the discharge is used to increase the plasma density at a rate proportional to the increase in power.

I. INTRODUCTION

Thin films of biomaterials are often used to line products that need to come in contact with living tissues. They are often found in prosthetics, bone plates, pins, rods, artificial heart valves, drug delivery devices, and many other products that need to be accepted by the body (Parida, Behera, Mishra, 2012). These thin films are created through a process called Plasma-Enhanced Chemical Vapor Deposition. In this process, the plasma dissociates the gas causing chemical reactions that can lead to the creation of reactive molecules which deposit on the surface of a substrate producing thin films of biomaterials. The goal of our research is to gain an understanding of these processes and their influence on the production of thin films. This could lead to the optimization of the production of these films in the future.

The electron energy distribution is the dominating factor behind the dissociation processes in H_2 plasma (Nunomura, S. and Kondo, M. 2007). The rate at which these processes occur is

$$V_a = C\int_{E_a}^{\infty}\sigma(E)f(E)dE, \tag{1}$$

where E_a is the threshold energy for the process to occur, $\sigma(E)$ is the cross-section, and $f(E)$ is the electron energy distribution described by

$$f(E) = A\frac{E}{T_e^{3/2}}e^{-E/kT_e}, \tag{2}$$

Where T_e is the electron temperature and E is the electron energy.

In order to model the electron temperature, the electron energy distribution is often assumed to be maxwellian (Figure 1.) By measuring the electron temperature, we can better understand the electron energy distribution that drives the ionization and dissociation of the gases leading to the chemical reactions and the rates at which these processes occur.

II. METHODS

A. POWER MEASUREMENT

Our system consists of a low pressure chamber with a powered electrode and a grounded electrode. Using a vacuum pump, our chamber is brought down to pressures of on the order of 10^{-7}mTorr. At this point, mass flow controllers are used to flow gas into our system. Then, a RF, radio frequency of 13.56MHz, power supply at is applied to the powered electrode and a discharge is ignited (Figure 2.) The circuit of our system consists of the power supply, matching network, and the chamber discharge. The matching network is a circuit configuration used to optimize the power delivered to the discharge by minimizing the power reflected to the power supply.

In order to correctly interpret plasma models, we need an accurate measure of the average power delivered to the discharge. As it turns out, the in-line power meters on the power supply are known to be inaccurate, as a result of losses in the matching network. A better approach to accurately measuring the average power is to probe the circuit directly before the powered electrode (Figure 3.) We collect the current and voltage near the top electrode using a digital oscilloscope and then transfer the data over to the computer for manipulation and analysis.

We can determine the average power delivered to the discharge with the current and voltage as function of time by

$$P_{ave} = \frac{1}{nT}\int_0^{nT} V(t)I(t)dt, \tag{3}$$

where *V(t)* is the voltage as a function of time and *I(t)* is the current as a function of time.

B. LANGMUIR PROBE MEASUREMENT

A Langmuir probe is an intrusive device that probes the plasma and collects information about the electron temperature, plasma density, and the plasma potential. The probe itself is a thin wire that probes the center of the plasma discharge (Figure 4.) We can measure an IV curve for an ideal probe and ideal plasma (Figure 5) by measuring the current as a function of time collected by the probe. Applying a very negative voltage leads to the collection of positive ions. As we increase the voltage, the probe begins to repel ions and collect electrons. At some point, the floating potential, the electron current and the ion current are exactly equal and there is no net flow of current. If the current is increased from here, electrons are collected at an exponential rate until electron saturation is reached. At this point electrons cannot be collected at a faster rate. The intersection between the exponential collection region and the electron saturation measures the plasma potential.

Using this IV curve, the electron temperature can be measured in two different ways. The first method is by fitting the exponential collection of electrons and determining the slope of this region. The electron temperature is determined by the inverse of the exponential slope. The second method of calculating the electron temperature is by relating the floating potential, plasma potential, and the ratio of the masses of the ions and electrons in the following way,

$$V_f = V_p + \frac{KT_e}{e}\ln\left(0.6\sqrt{\frac{2\pi m_e}{m_i}}\right), \tag{4}$$

Where V_f is the floating potential, V_p is the plasma potential, T_e is the electron temperature, m_e is the mass of an electron, and m_i is the mass of the ions.

III. RESULTS AND DISCUSSION

In order to accurately measure the power delivered to the discharge, we need to measure the current and voltage as a function of time. This will allow us to calculate the average power delivered to the discharge using Equation 4. However, the first power measurement that we take is with the discharge off. With the discharge off, we would expect the chamber to act as a purely capacitive load. This is a result of the chamber plates acting as a parallel plate capacitor and the stray capacitance of the walls of the chamber and the grounded shield above the powered electrode. This purely capacitive load should result in the current and voltage completely 90 degrees out of phase and zero average power. However, we see from the measurement that with the discharge off, there is roughly a 85 degree phase shift and an average power is measured. At frequencies on the order of 10MHz, we see delays in the propagation of the current and voltage probe and it is the difference in the delays that lead to this phase shift away from 90 degrees. In order to compensate for this phase shift, we simply shift the current over until the integral of the average power delivered is zero and the current and voltage are 90 degrees out of phase. Then, we have the current and voltage measurements as a function of time (Figure 6.) We measured the current and voltage as a function of time at 15 watts of nominal power read off the power supply (Figure 7.)

We can plot of actual power as a function of the nominal power (Figure 8) and our measurements indicate that roughly 75% to 80% of the nominal power is dissipated before reaching the discharge. This loss in power is often assumed to be a result of skin effects in the inductor of the matching network. Essentially, the skin effects are eddy currents in the surface of the wire of the inductor. This is confirmed in our system as our inductor is discolored and often hot after longer periods of data collection. Our data confirms the notion that the nominal power read off of the power supply is inaccurate and probing the system directly before the powered electrode gives a much more accurate measure of the power delivered to the system.

With an accurate measure of power, we can compare the effects of the power delivered to the plasma with the electron temperatures in the plasma. Our IV curve is consistent with an ideal IV curve (Figure 9) until it reaches the electron saturation region. At this point, a couple non-ideal effects in the plasma begin to take place. First, at these high voltages the probe starts to experience heating effects. Secondly, at voltages above the plasma potential, the probe begins to perturb the plasma, changing the characteristics of the plasma near the probe. The electron saturation region of the curve is usually only used to find the plasma potential as a result of these non-ideal effects (Merlino, R. 2007) that occur at voltages beyond the plasma potential. Using Equation 2, we can use the inverse of the slope of the exponential fit of the electron collection region to calculate the electron temperature (Figure 10.) In this case, we measure an electron temperature of 5.56eV.

We can also find the electron temperature the alternative way, Equation 4, and compare results for consistency. Table 1 gives the plasma potential and floating potential from the IV curves at multiple nominal powers. Comparing the measured electron temperature using the two different methods (Figure 11,) our data is self-consistent and measures electron temperatures near 6eV. It appears that as we increase the nominal power to the discharge the electron temperature remains constant.

By relating the current at voltages much less than the plasma potential, we can better understand the effect of increasing the power. Our data suggest that the increase in power results in an increase in the plasma density. We measure the ion current at voltages much less than the plasma potential of the IV curve for different actual powers (Figure 12.) At voltages much less than the plasma potential, we expect the plasma density to be proportional to the actual power delivered to the discharge and this is consistent with our measurements.

IV. SUMMARY AND CONCLUSION

Analysis of the power measurement confirms the idea that the nominal power read off of the power supply is inaccurate and a better approach to measuring the true power delivered to the discharge is by probing the system directly before the top electrode. Our data shows 75% to 80% of the power is lost before reaching the discharge. The discoloration of the inductor in our matching network is consistent with the idea that a majority of the power is lost due to skin effects in this inductor (Niknejad, I.M and Meyer, R.G. 2012).

We can also conclude that our discharge is highly capacitive. We notice that even after correcting for the delays in the probe that the current and voltage are almost 90 degrees out of phase. These small phase shift from discharge off to discharge on are very sensitive and a reactive circuit can be added to cancel some of the stray capacitance in the system. However, there is a trade off as the reactive circuit contains an inductor which could produce addition losses in power due to skin effects.

We conclude from our Langmuir probe data that the electron temperature remains constant around 6eV even as we vary the power applied. Our data does suggest that the additional power is used to increase the plasma density rather than the electron temperature.

In the future, we may be able to increase the accuracy of the electron temperature by improving the assumption that the electron energy distribution is maxwellian and consider a bi-maxwellian instead. This distribution would contain two groupings of electron energies. One at lower electron energy and another at higher energy, but this will take more research and investigation.

REFERENCES

Merlino, R. 2007 American Association of Physics Teachers, **1**, 1081

Niknejad, I.M and Meyer, R.G. 2012 IEEE TRANSACTIONS ON MICROWAVE THEORY AND TECHNIQUES, **49**, 172

Nunomura, S. and Kondo, M. 2007 JOURNAL OF APPLIED PHYSICS **102**, 2

Parida, P. Behera, A. Mishra, S.C. 2012, International Journal of Advances in Applied Sciences, **1**, 31

TABLES

Nominal Power (watts)	V_p	V_f
5	22.8	0.68
10	24.3	1.95
15	25.1	2.81
20	26.1	3.32

Table 1: Relationship between the power delivered to the discharge, the plasma potential, and the floating potential used to calculate the electron temperature.

FIGURES

Figure 1: An example of a maxwellian energy distribution.

Figure 2: Simple diagram of our chamber system. Note: In our system the powered electrode is the top electrode, but effectively they are equivalent.

Figure 3: Diagram of the current and voltage probes used to measure the true power delivered to the system.

Figure 4: Simple Langmuir probe circuit diagram.

Figure 5: Ideal plasma and probe IV curve collected to the Langmuir probe. Applying a very negative voltage leads to the collection of positive ions. As we increase the voltage, the probe begins to repel ions and collect electrons. At some point, the floating potential, the electron current and the ion current are exactly equal and there is no net flow of current. If the current is increased from here, electrons are collected at an exponential rate until electron saturation is reached.

Figure 6: Measured current and voltage as a function of time with the discharge off.

Figure 7: Measured current and voltage as a function of time with a 15 watt nominal power discharge.

Figure 8: A plot of the actual power delivered to the discharge as a function of the nominal power read off of the discharge.

Figure 9: A plot of the current as a function of voltage of the Langmuir probe.

Figure 10: A plot of the exponential fit to the electron collecting region in Figure 9.

Figure 11: A plot comparing the measured electron temperature from two different methods as a function of nominal power.

Figure 12: A plot of the current as a function of actual power delivered to the discharge. Note: In this region, we would expect the current to be proportional to the plasma density. Implying the plasma density increases linearly as a function of actual power.

Figure 1

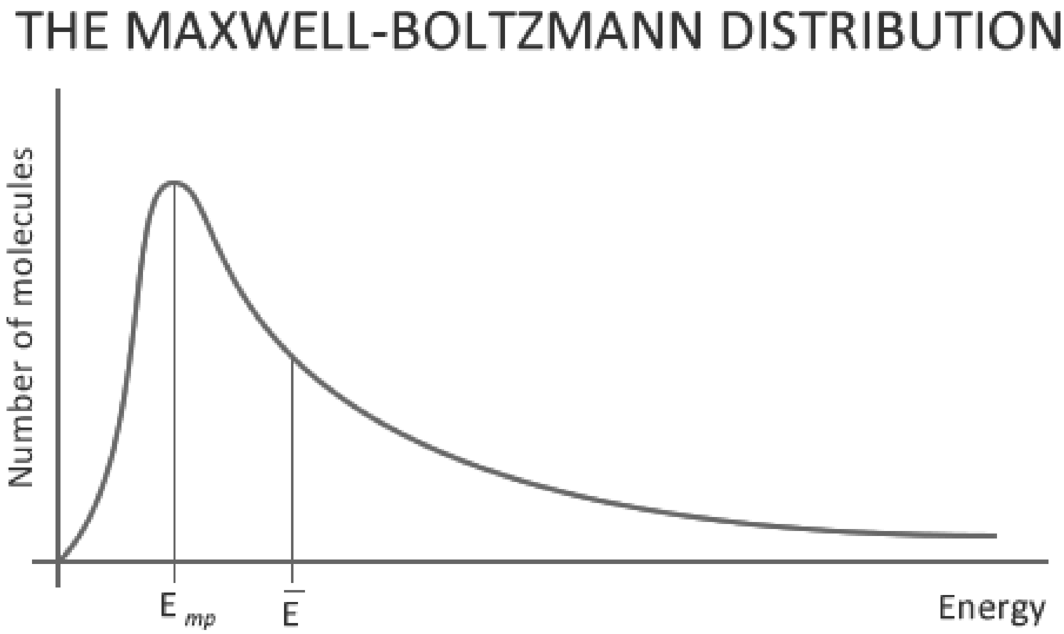

http://www.freezingblue.com/flashcards/print_preview.cgi?cardsetID=265934

Figure 2

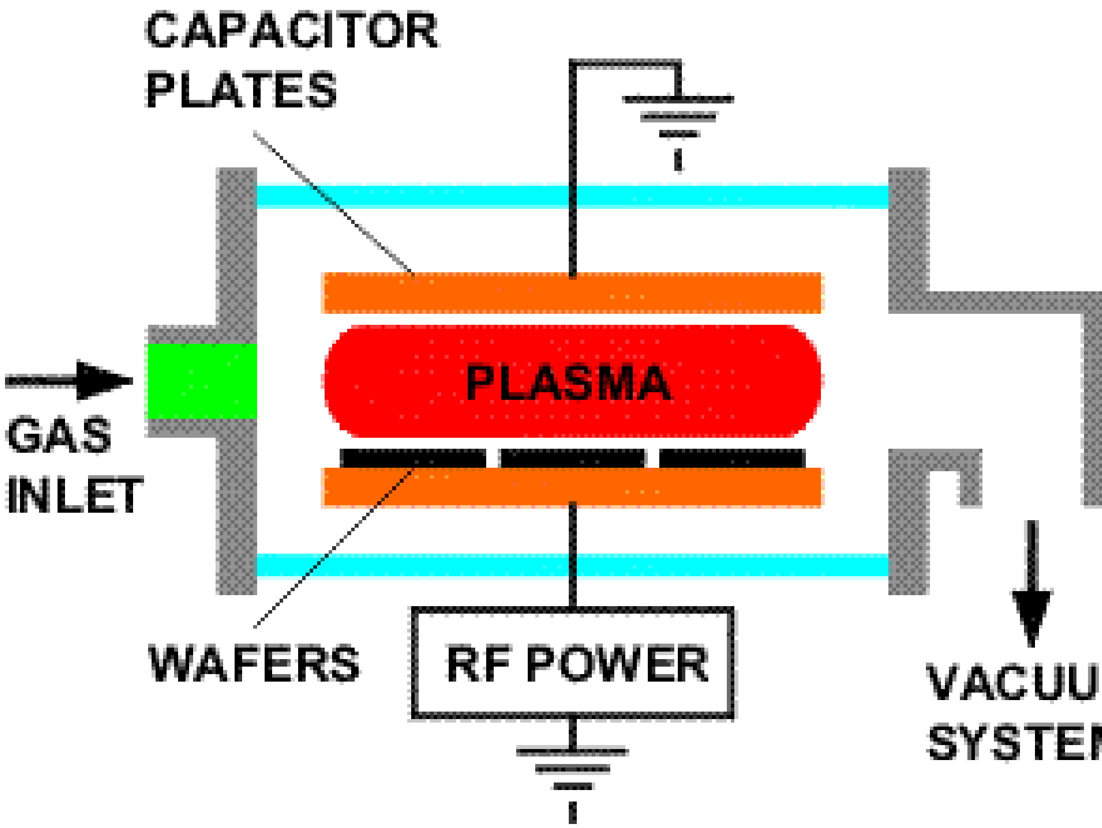
CAPACITOR
PLATES
PLASMA
GAS
INLET
WAFERS
RF POWER
VACUUM
SYSTEM

Figure 3

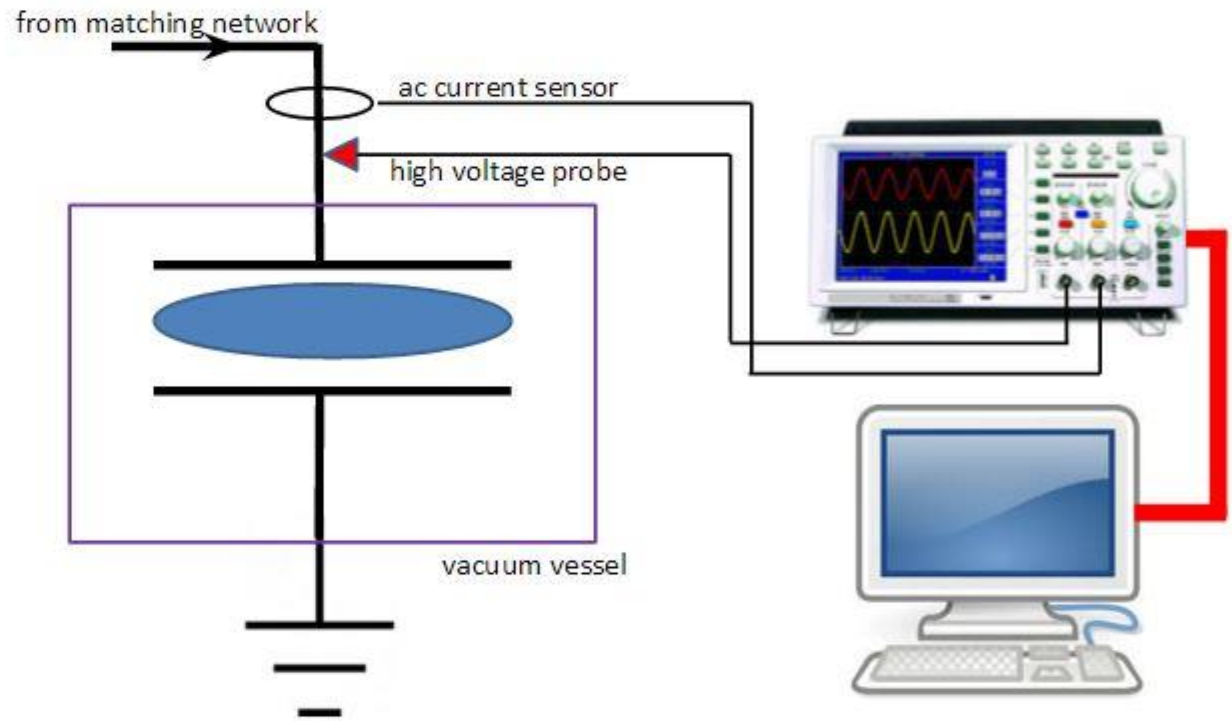
from matching network
ac current sensor
high voltage probe
vacuum vessel

Figure 4

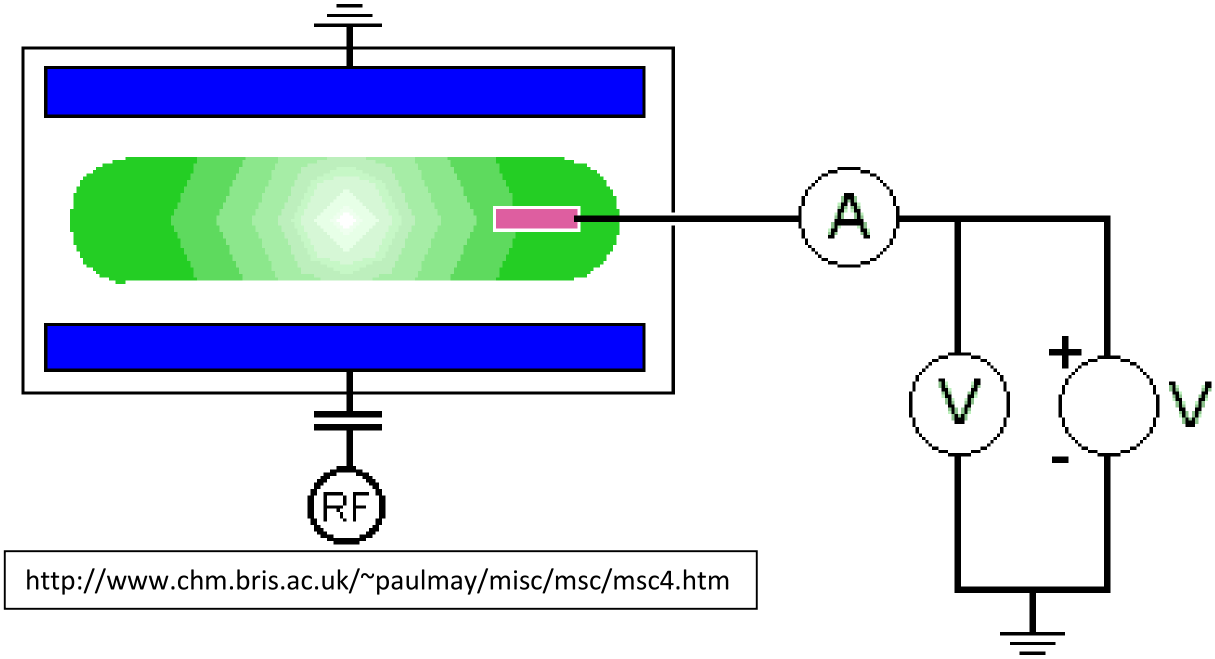

Figure 5

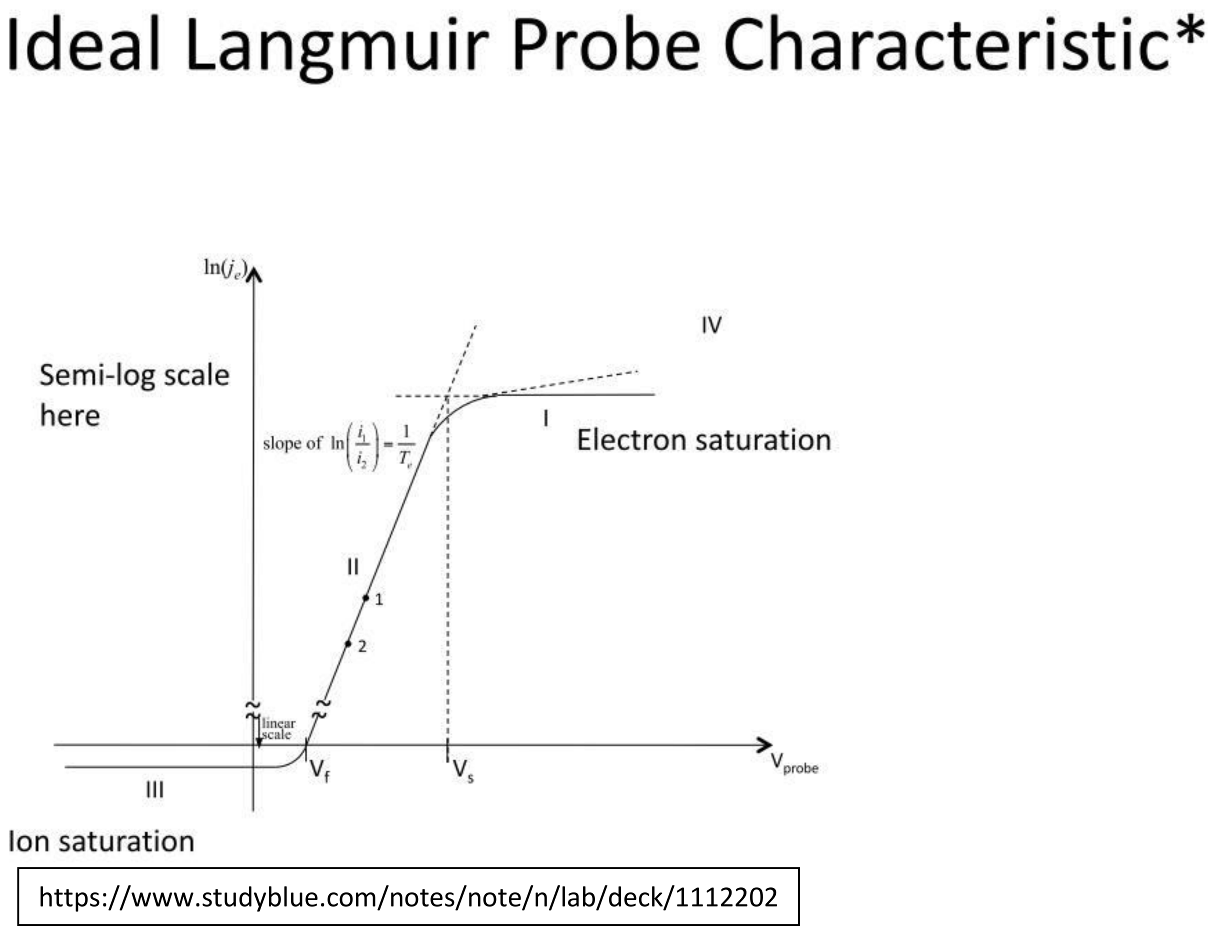

Ideal Langmuir Probe Characteristic*
ln(j_e)
Semi-log scale
here
IV
I
Electron saturation
slope of ln(i1/i2) = 1/Te
II
1
2
linear
scale
Vf
Vs
Vprobe
III
Ion saturation
https://www.studyblue.com/notes/note/n/lab/deck/1112202

Figure 6

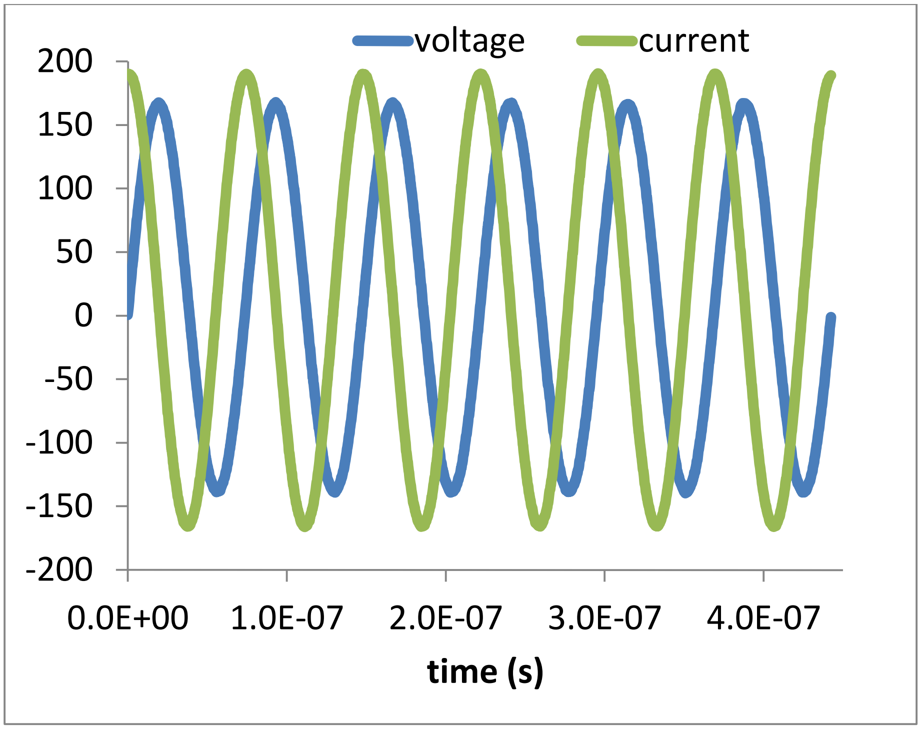
voltage
current
200
150
100
50
0
-50
-100
-150
-200
0.0E+00
1.0E-07
2.0E-07
3.0E-07
4.0E-07
time (s)

Figure 7

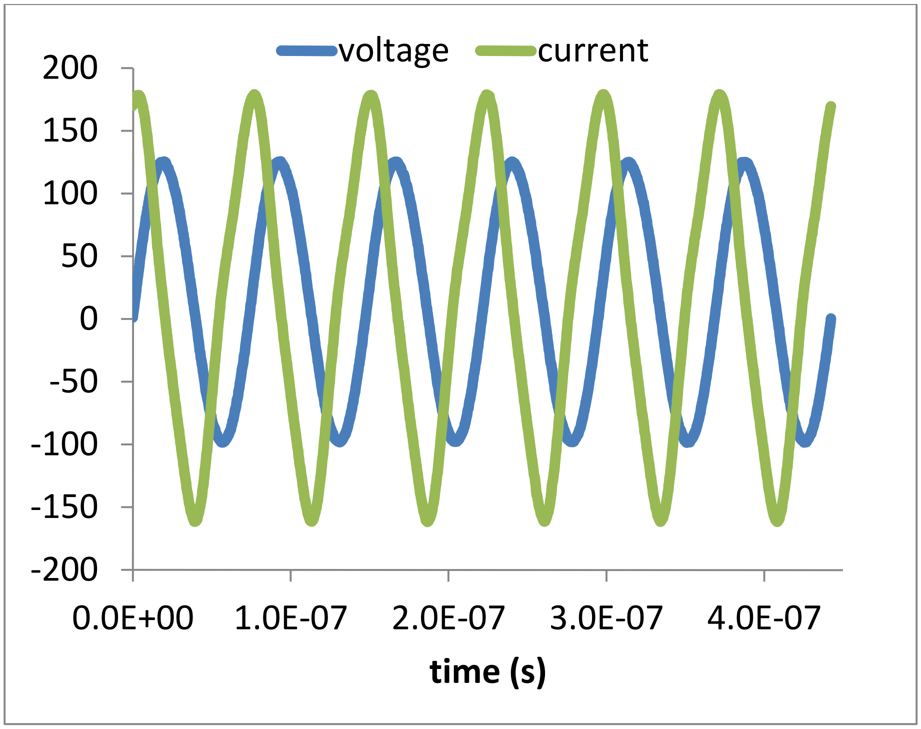
voltage
current
200
150
100
50
0
-50
-100
-150
-200
0.0E+00
1.0E-07
2.0E-07
3.0E-07
4.0E-07
time (s)

Figure 8

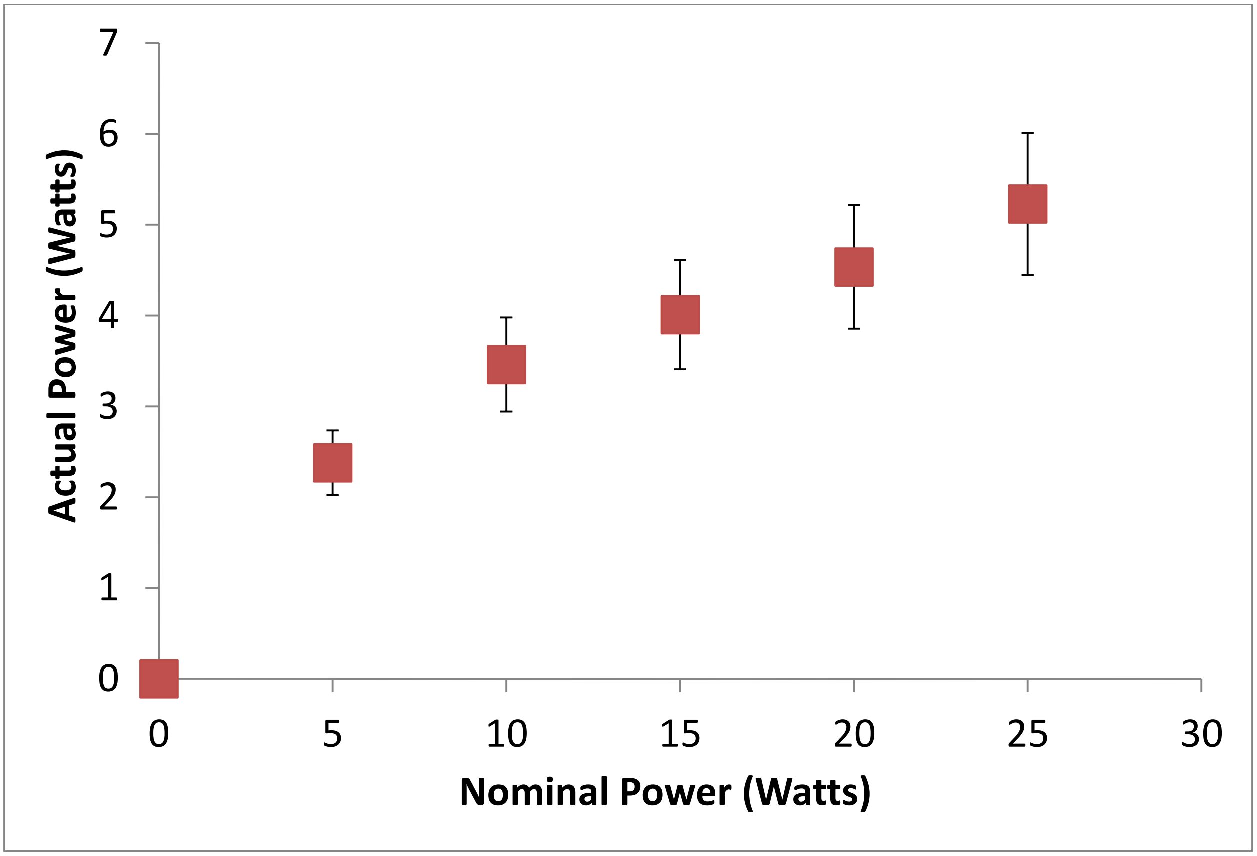
Actual Power (Watts)
7
6
5
4
3
2
1
0
0
5
10
15
20
25
30
Nominal Power (Watts)

Figure 9

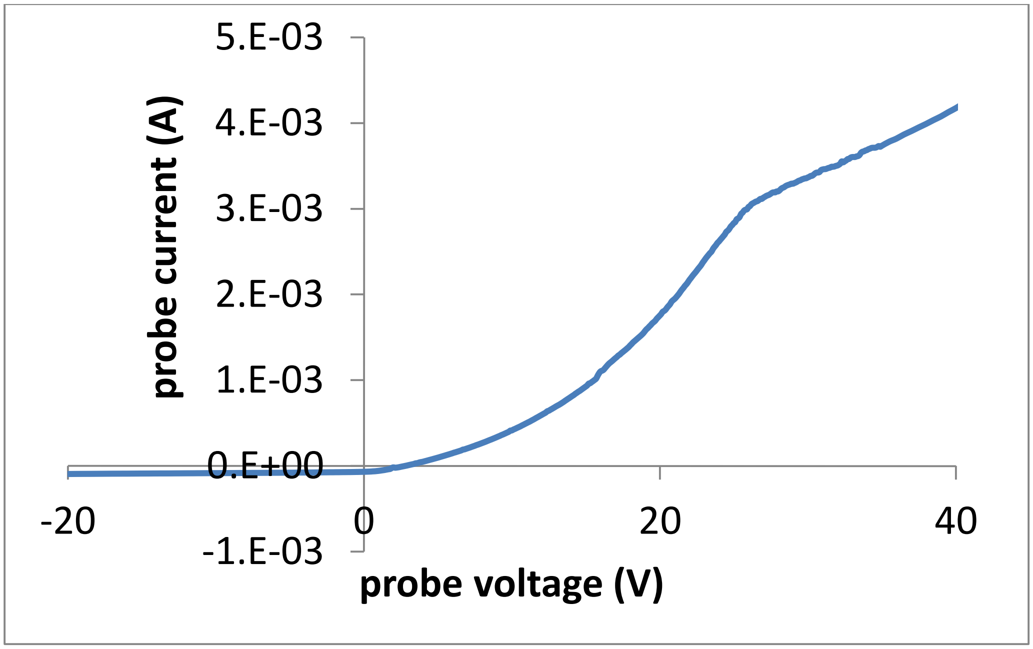
5.E-03
4.E-03
3.E-03
2.E-03
1.E-03
0.E+00
-1.E-03
probe current (A)
-20
0
20
40
probe voltage (V)

Figure 10

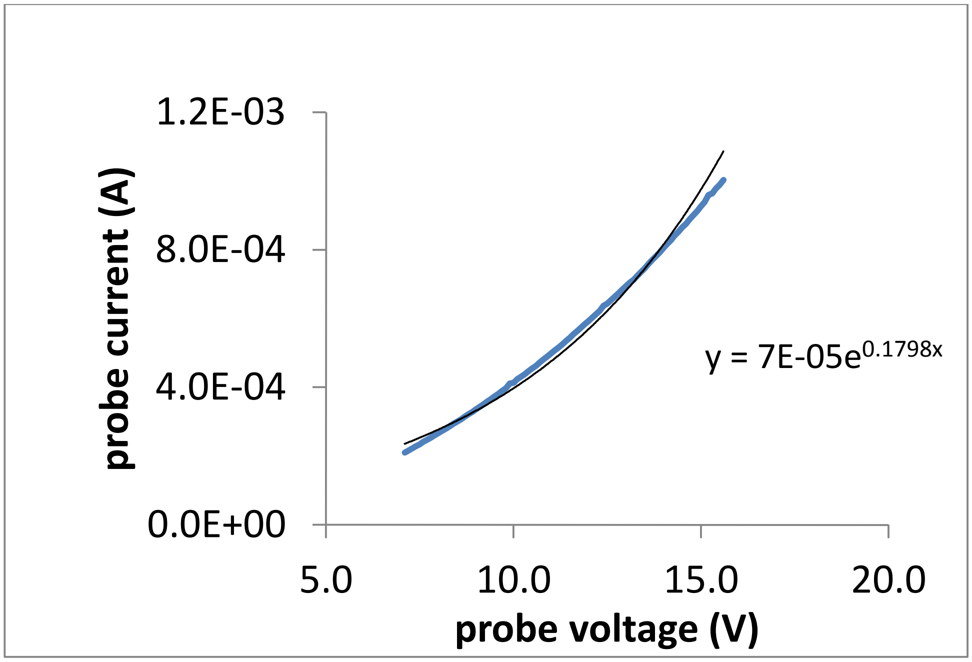
1.2E-03
8.0E-04
4.0E-04
0.0E+00
probe current (A)
5.0
10.0
15.0
20.0
probe voltage (V)
y = 7E-05e^0.1798x

Figure 11

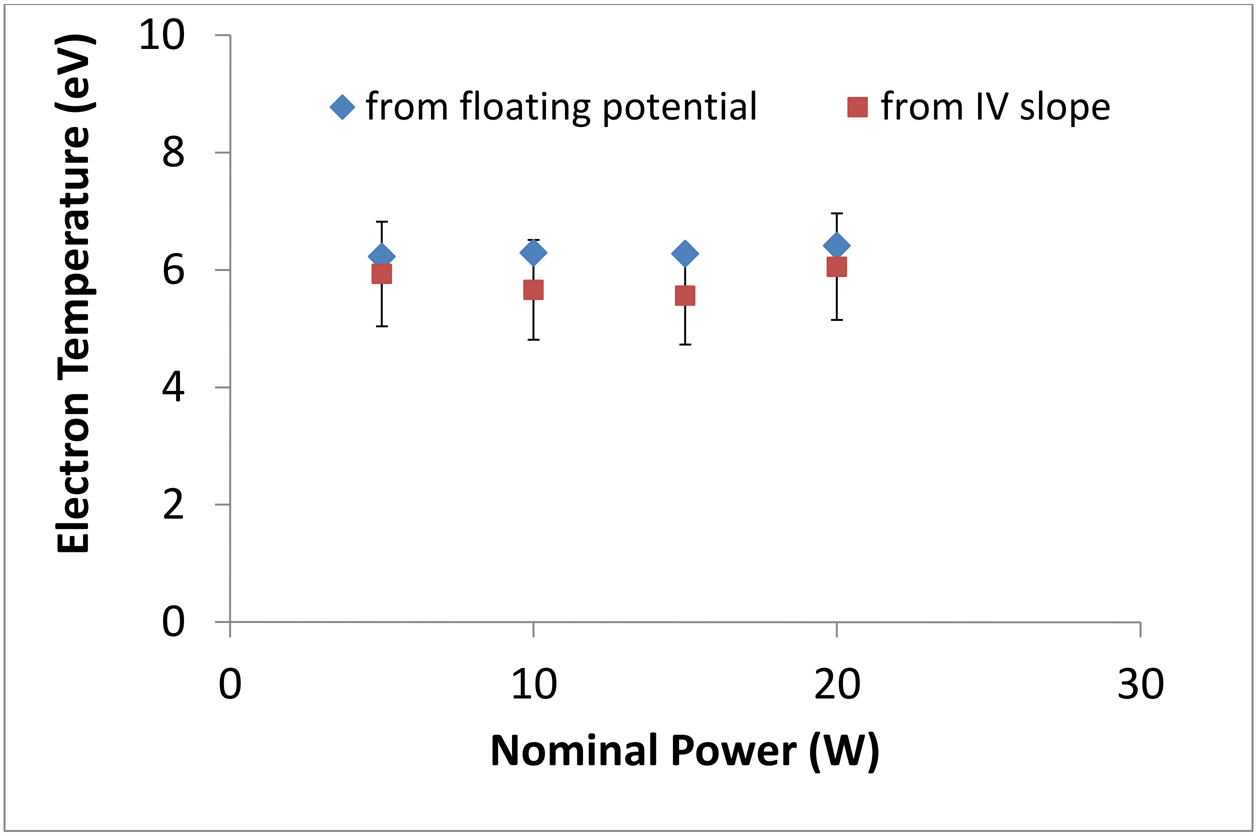
from floating potential
from IV slope
Electron Temperature (eV)
Nominal Power (W)
0
2
4
6
8
10
0
10
20
30

Figure 12

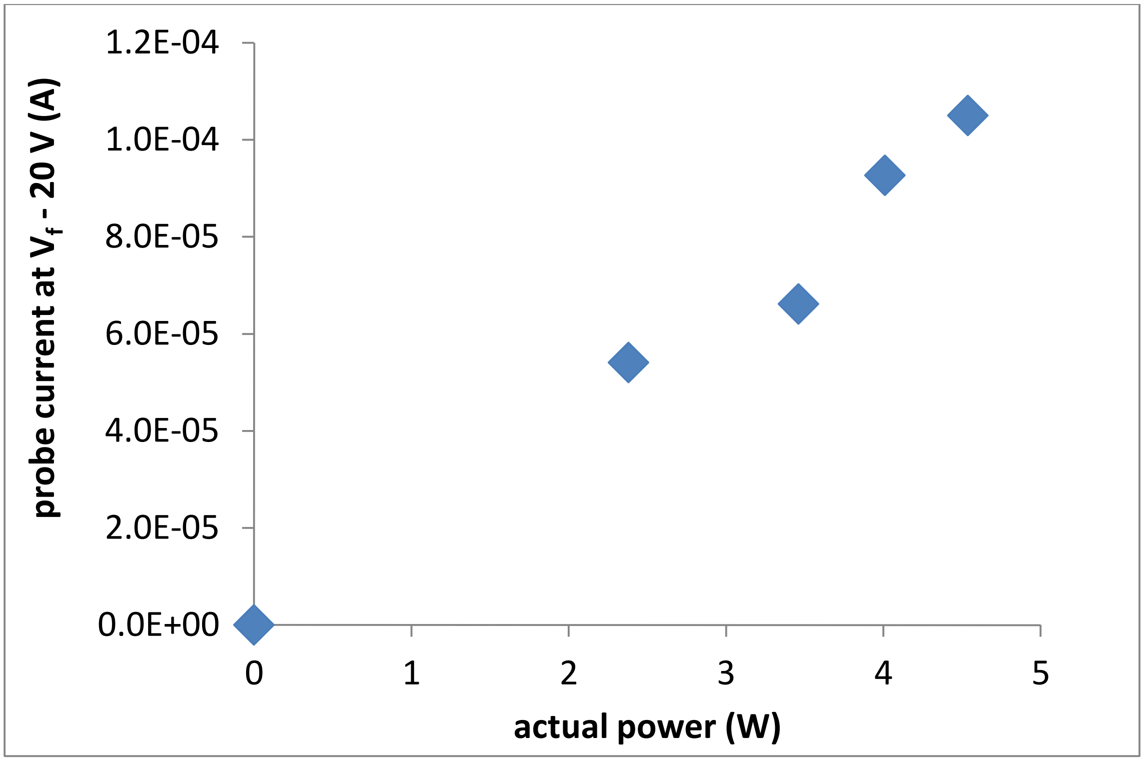
1.2E-04
1.0E-04
8.0E-05
6.0E-05
4.0E-05
2.0E-05
0.0E+00
0
1
2
3
4
5
probe current at V_f - 20 V (A)
actual power (W)